iMFREE: A versatile software tool for modelling machining processes with particle methods

Originally published in:
Procedia CIRP 117, https://doi.org/10.1016/j.procir.2023.03.004

Funding acknowledgement:
149436 - GPU-Enhanced Metal Cutting Simulation using Advanced Meshfree Methods (SNF)

Available online at www.sciencedirect.com

ScienceDirect

Procedia CIRP 117 (2023) 13–19

www.elsevier.com/locate/procedia

19th CIRP Conference on Modeling of Machining Operations

iMFREE: A versatile software tool for modelling machining processes with particle methods

Hagen Klippel[a,*], Nanyuan Zhang[a], Michal Kuffa[a], Mohamadreza Afrasiabi[b], Markus Bambach[c], Konrad Wegener[a]

[a]*Institute of Machine Tools & Manufacturing, ETH Zurich, Leonhardstrasse 21, 8092 Zürich, Switzerland*
[b]*Data-Driven & Computational Manufacturing Group, inspire AG, Technoparkstrasse 1, 8005 Zürich, Switzerland*
[c]*Advanced Manufacturing Lab, ETH Zurich, Technoparkstrasse 1, 8005 Zürich, Switzerland*

* Corresponding author. Tel.: +41-44-632-9479 ; fax: +41-44-632-1125. *E-mail address:* klippel@iwf.mavt.ethz.ch

Abstract

The current state-of-the-art for the simulation of machining process is the application of the FEM (finite element method). Nevertheless, the cost of FEM analyses for such problems is high due to their complex multi-physics nature, mesh regeneration issues, and small time-length scales. In contrast, particle methods are an alternative numerical approach well-suited for large deformations as in material's chip formation. In this work, the key features and simulation capabilities of iMFREE are presented, which is a massively parallel and robust particle-based code for machining simulations developed at the ETH Zürich. Various applications of iMFREE are shown, where the efficiency is demonstrated in orthogonal cutting simulations for the optimisation of material removal rates, a chip formation study, the inverse identifications of friction law parameters and material constitutive law parameters. Further, the applicability to single and multiple grain grinding simulations of Ti6Al4V and silicon is shown.

Keywords: Machining; Metal Cutting; Modeling; Simulation; Particle Methods; SPH; FEM; SPH-FEM coupling; Graphics Processing Unit (GPU).

1. Introduction

The numerical simulation of machining processes is a demanding task since the modelling of the material behaviour [1] and choosing a numerical method to discretise the continuum [2] have not yet been conclusively resolved. Mostly, the finite element method (FEM) is used for numerical machining simulations. The FEM is a versatile and mature tool, but frequent remeshing is required to cope with large deformations and material separations during the simulation of machining processes. Since the time consuming remeshing operations hamper the performance of FEM-codes, alternative numerical methods, which do not rely purely on a mesh, are an attractive candidate for machining simulations. Examples for such methods are the Particle Finite Element Method (PFEM) in [3], the Material Point Method (MPM) in [4] or the Smoothed Particle Hydrodynamics (SPH) which utilizes no mesh but particles only. In SPH, particles move with the continuum and easily handle large deformations. In [5], it is shown that SPH is well suited for parallelisation on the GPU because of the large amount of computations due to particle interactions and enables short runtimes of machining simulations.

This report begins with a brief introduction into the SPH method, followed by a demonstration of the SPH package iMFREE which is currently developed at IWF at ETH Zürich.

Nomenclature

CSPM	Corrective Smoothed Particle Method
DOE	Design Of Experiments
FEM	Finite Element Methods
GPU	Graphics Processing Unit
JC	Johnson Cook
ML	Machine Learning

* * Corresponding author. Tel.: +41-44-632-9479 ; fax: +41-44-632-1125.
E-mail address: klippel@iwf.mavt.ethz.ch

10.1016/j.procir.2023.03.004

MPM	Material Point Method
MRR	Material Removal Rate
PFEM	Particle Finite Element Method
RKPM	Reproducing Kernel Particle Method
SPH	Smoothed Particle Hydrodynamics
SSL	Shear Stress Limit

2. Theoretical Background

SPH was introduced 1977 in astrophysics for the calculation of a smoothed density from point clouds [6]. The method can be derived from the partition of unity [7], where a field value at a spatial location x can be determined as:

$$f(x) = \int_{\mathbb{R}^d} \delta(x - x') f(x') d\Omega_{x'} \qquad \forall x \in \mathbb{R}^d \tag{1}$$

The Dirac delta function $\delta(x)$ in equation (1) has two important properties:

$$\int_{-\infty}^{+\infty} \delta(x) dx = 1 \tag{2}$$

and

$$\int_{-\infty}^{+\infty} \delta(\zeta - x) f(\zeta) d\zeta = f(x) \tag{3}$$

Replacing the Dirac delta function δ with a smoothing function, the so called Kernel, $W(x - x, h)$, e.g. the Gauß-function, with h being a smoothing length, the behaviour of the Dirac delta can be reproduced for the limit:

$$\lim_{h \to 0} W(x - x', h) = \delta(x - x') \tag{4}$$

Inserting (4) into equation (3) gives an approximation of the function value $f(x)$ at x:

$$< f(x) >= \int_{-\infty}^{+\infty} W(x - x', h) f(x') dx' \tag{5}$$

This can be approximated within a discrete neighborhood using a Riemann-sum:

$$< f_i >= \sum_j f_j W(x_{ij}, h) \Delta V_j \tag{6}$$

with the point index i at which the function value is to be approximated by its neighbour points j, x_{ij} is the spatial distance between point i and j and ΔV_j being an integration weight of point j. Approximation of the function's derivative leads to

$$< \nabla f_i >= \sum_j f_j \nabla W(x_{ij}, h) \Delta V_j \tag{7}$$

where only the derivative of the Kernel $W(x_{ij}, h)$ is required. Thereby, derivatives of values given at point cloud locations can be computed without the requirement of a functional description or a mesh-based relation between these points (particles). With this meshfree approximation derivatives in continuum mechanics equation can be computed by sums of discrete values in the particle's neighborhood. Meshfree techniques were adopted in early 1990s to structural simulations [8] and for numerical cutting simulations first by [9].

At IWF of ETH Zürich the software tool iMFREE was developed by Röthlin [10] in the past years for SPH based machining simulations. The software is capable of performing CPU as well as GPU-enhanced computation of metal cutting simulations. It facilitates the most recent correctors, e.g. CSPM and RKPM, and stabilisation measures for mechanical [11] and thermal simulations [12] with various material models [13]. Comparison and validation computations between SPH and FEM are conducted in [11] for a tension test and a rubber ring impact simulation. A recomputation of a SHTB test specimen with SPH is shown in [13] where the results are compared against FEM and experimental results conducted in [14, 15].

3. Simulation Examples

A selection of machining operations simulated with iMFREE is given in the following. First, computationally highly efficient metal cutting simulations in 2D are shown, followed by some 3D applications to single and multiple grain grinding of Ti6Al4V and diamond wire sawing of silicon.

3.1. Orthogonal Cutting Simulations

The orthogonal cutting mode is often used in numerical simulations since it can be efficiently approximated with the 2D plane strain assumption. Using GPU acceleration, the rapid determination of process forces becomes possible and thus can be used as a basis for optimisations, for example tool wear

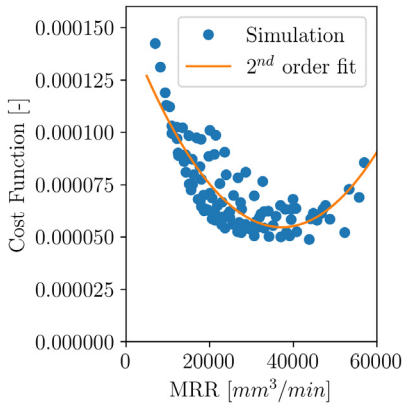

Fig. 1. Optimisation of a Ti6Al4V cutting process with regards to material removal rates and wear, from [5].

optimisation or parameter identifications. Furthermore, high-resolution simulations can be performed, which allow deeper insights into the chip formation process. In the following, some examples of such simulations conducted with iMFREE are presented.

3.1.1. Optimisation of Material Removal Rates

In [5], iMFREE is applied to the simulation of 1 mm cutting length with a discretisation of ≈ 6′000 SPH particles. Due to the GPU acceleration the runtime was only about 20 min. Similar simulations on a single CPU core required in the past about 70 h for completion, when using the SPH in LS-Dyna [16]. The speed-up enabled to run a prototype cutting process optimisation simulation, where a cost function is optimised with regards to material removal rates (MRR) and wear. The optimisation was run for 100 different combinations of feed rates f and cutting speeds v_c using 2'500 particles and took 37 h on a NVidia Tesla P100 GPU. Figure 1 shows the simulation results together with an approximation by a quadratic function, which shows a clear global minimum of the cost function.

3.1.2. Chip Formation Study

The computing power of the NVidia Tesla P100 can be exploited by using a large number of particles, which enables a better resolution of possible shear bands, as proposed in [17]. For that purpose, the chip shape formation was studied in Ti6Al4V cutting using 150'000 particles. By this, the thermal softening can be identified as the mechanism for shear banding, which gives rise to serrated chips. Counteracting is the thermal conductivity, which dissipates the heat developed by plastic flow and thus removes the nearly adiabatic shear bands, see Figure 2. This indicates that the softening predicted by the JC flow stress model is not sufficient.

3.1.3. Identification of Friction Parameters

Based on experimental observations on Ti6Al4V cutting experiments using an in-process tribometer, a temperature dependent friction coefficient $\mu(T)$ is identified using 375 orthogonal cutting simulations in [18]. The temperature-dependent friction

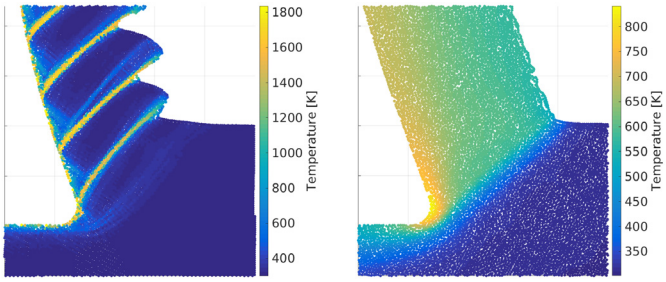

Fig. 2. Predicted temperature distributions in high resolution orthogonal cutting simulations of Ti6Al4V using the standard Johnson Cook flow stress model. Simulation without (adiabatic, left) and with (right) heat conduction, from [5].

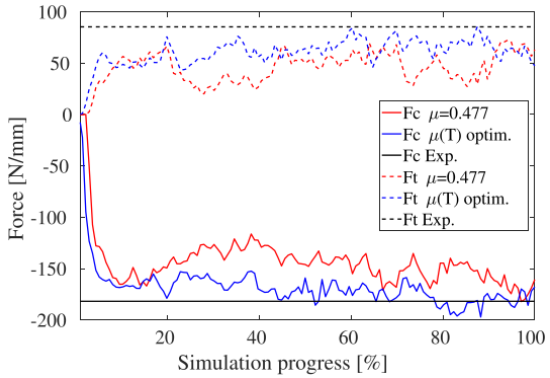

Fig. 3. High resolution orthogonal cutting simulation of Ti6Al4V using the standard Johnson Cook flow stress model without (left) and with (right) heat conduction, from [5].

model introduces a parameter q to describe the temperature dependency:

$$\mu(T) = \mu_0 \left[1 - \left(\frac{T - T_r}{T_m - T_r} \right)^q \right] \tag{8}$$

where T is the current temperature, T_{ref} the reference temperature and T_m is the melting temperature.

With the obtained parameters for the temperature-dependent friction law, the errors of the force prediction were significantly decreased, which is displayed in Figure 3. It is however concluded, that further improvements can be achieved, if the friction parameter identification is performed together with the material constitutive law parameters within an instrumented orthogonal cutting test.

3.1.4. Inverse Parameter Identification of Material Constitutive Law Parameters

In [13] iMFREE was used for inverse parameter identification of constitutive model parameters of Ti6Al4V and Ck45 using the Johnson-Cook [19] flow stress model. Measured process force components of quasi-orthogonal cutting experiments from [20] were used to drive the parameter identification using

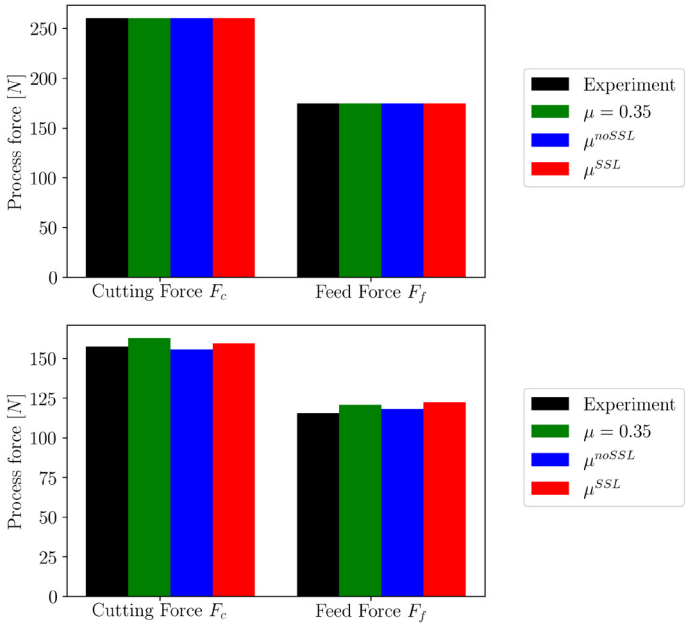

Fig. 4. Comparison of experimental and numerical process forces obtained with material parameters from an inverse parameter identification using different assumptions for the friction coefficient for Ck45 (top) and Ti6Al4V (bottom), from [13].

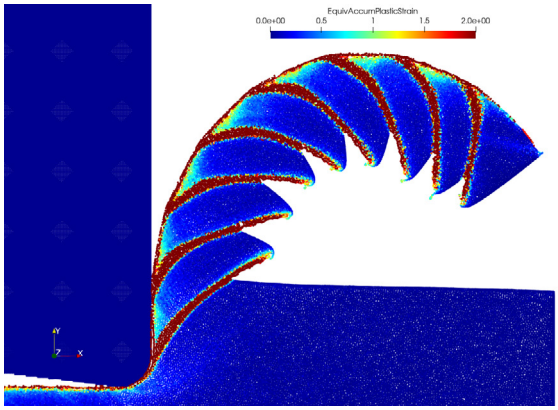

Fig. 5. High resolution orthogonal cutting simulation of Ti6Al4V using the standard Johnson Cook flow stress model with heat conduction in tool and workpiece, from [13].

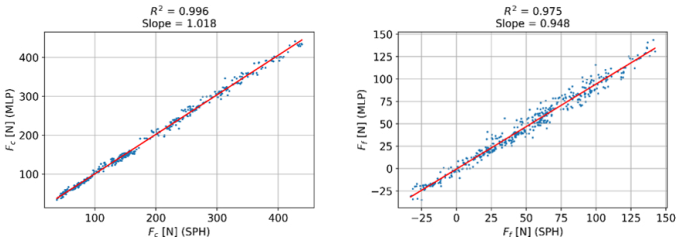

Fig. 6. Residuals in the cutting (left) and feed force (right) preditions, from [24].

a genetic algorithm. For friction modelling, three assumptions were made:

1. constant Coulomb friction coefficient $\mu = 0.35$
2. constant Coulomb friction coefficient identified together with the 5 JC parameters, without shear stress limit (SSL)
3. constant Coulomb friction coefficient identified together with the 5 JC parameters, with SSL: the frictional shear stress is limited to the current yield stress of the material

All three friction assumptions lead to very good agreements between experimentally measured and numerically predicted process forces for Ck45 and Ti6Al4V, which is displayed in Figure 4.

For efficiency reasons, a rather compact numerical model with 5'640 particles with a particle spacing of 10 μm and without tool-workpiece heat transfer was used in the parameter identification procedure yielding in runtimes of about 3 to 4 minutes on scientific GPUs. This resolution is however not sufficient for the prediction of chip segmentations, since the primary shear zone layer thickness is in the order of 2...6 μm as shown in [13]. Therefore, the resolution of the numerical simulation was massively increased to be able to resolve the shear localization. A particle spacing of about 1.5 μm was used, the tool-workpiece heat transfer was switched on, and in contrast to the findings in chapter 3.1.2, chip segmentation can be clearly seen in Figure 5, even with heat conduction. The findings reveal that extensions of the JC flow stress model, e.g. those introduced by [21, 22, 23], are not required to enable shear localizations in the chip and therefore chip segmentations.

3.1.5. *Process Force Prediction Using ML*

A process force prediction tool for orthogonal cutting of Ti6Al4V was proposed in [24], based on a machine learning model. In contrast to analytical approaches, e.g. based on the Oxley model [25] or its extensions [26], not just feed f, cutting speed v_c and rake angle γ can be considered but also the cutting edge radius r_n and the clearance angle α. Instead of learning from cutting experiments, virtual experiments are conducted based on SPH simulations with iMFREE within a DOE with 2'500 orthogonal cutting simulations. The virtual experiments avoid time consuming cutting experiments with different cutter geometries and process conditions. Due to the massive parallelisation the simulations were computed within just five days using five GPUs.

The ML model computations are very fast thus enabling 100 evaluations per second, which makes it attractive to be used in the optimization of cutting processes. Figure 6 shows the residuals for the cutting and feed force predictions versus the SPH predictions. Obviously, the feed force component is predicted with a lower accuracy than the cutting force component.

The ML based process force model is used for predictions which are compared with real experiments conducted by [27]. In Figure 7 it can be seen that the trends of the specific cut and feed force are captured well over a range of different feed rates, but with smaller magnitudes than experimentally observed. In general, the cutting forces are predicted with lower deviations than the feed forces when compared to the experimental results. From these findings it is concluded that on the one hand the ML model itself needs further scrutinies to improve the predictional

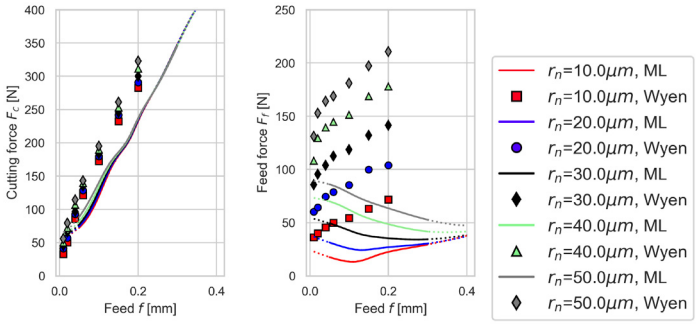

Fig. 7. Cutting and feed force predictions with the ML model compared to experimental results [27], from [24].

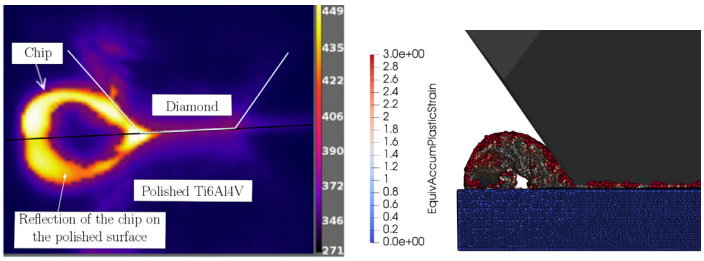

Fig. 8. Grinding of Ti6Al4V with strongly negative rake angle: experiment (left) and simulation (right) showing chip curling, from [28].

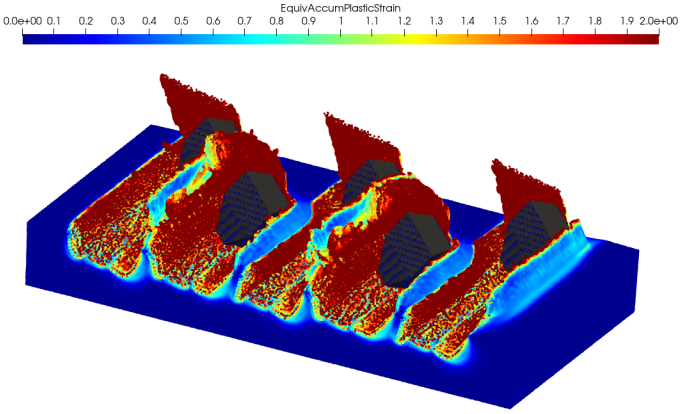

Fig. 9. Ti6Al4V grinding simulation with 5 diamond grains, from [28].

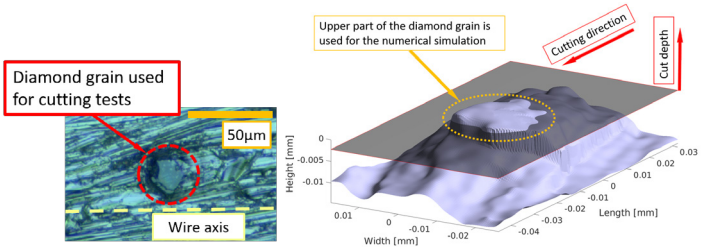

Fig. 10. Grinding of silicon: microscope image from diamond grain on wire (left) and 3D scanned surface of the diamond grain (right) with the marked area used for the diamond grain model, from [31].

performance. On the other hand the deviations in the process forces hint that the constitutive modelling in the numerical simulations requires improvements to be able to cover large ranges of process conditions and different tool geometries.

3.2. 3D Simulations

3.2.1. Grinding

In [28], the first full-scale single grain simulation using meshless methods was demonstrated. This became possible due to massive parallelisation using GPU computing. In the past, [29] had to introduce a scaling of the tool geometry and locally refitted material parameters to enable such computations at all. Using the CSPM correction scheme for SPH, it was possible to numerically simulate the experimentally observed chip curling. A comparison of the experimental and the numerically simulated chip shape is shown in Figure 8.

Additionally, the interaction between diamond grains of engineered grinding tools is studied in a simulation using a resolution of 1.5 million particles, which is shown in Figure 9. This is the - so far - largest published metal cutting simulation with a runtime of about 20 hours. Compared to single grain simulations published in [30], this is a 90 times performance increase. It is shown that considerable wear effects are to expect when subsequent grains have overlapping paths, because the trailing grain comes into contact with pre-hardened material.

3.2.2. Silicon Scratching

In this study [31], single diamond grain cutting experiments in the ductile mode were simulated with iMFREE in 3D and compared to experimental results. The diamond grain used in the cutting experiments was scanned prior to the tests with the focus variation principle. The resulting 3D geometry shown in Figure 10 was then used to create a numerical model of the diamond grain for the numerical simulation. Since the JC flow stress model was used, the analyses only have limited validity in the ductile range, i.e. up to depths of cut that lay in and above the ductile-to-brittle transition. At higher cutting depths, phase transformations of the silicon are to be expected due to hydrostatic pressures exerted from the tool to the silicon. An example hydrostatic pressure distribution is provided in Figure 11 together with the residual scratch depth distribution due to elastic recovery. In the simulations, the cutting forces were predicted to be only slightly higher, while the normal forces were significantly overestimated. This could be due to the material model used, since the density changes occurring due to phase transformations cannot be represented.

4. Summary and Outlook

In this paper, a summary of various 2D and 3D simulations using iMFREE has been given, showing its superiority over conventional numerical methods in modelling machining operations. Firstly, very short computing times for machining simulations can be realised through parallelisation on the GPU, which can be exploited advantageously for optimisations. This was demonstrated in a MRR optimisation and in the identifi-

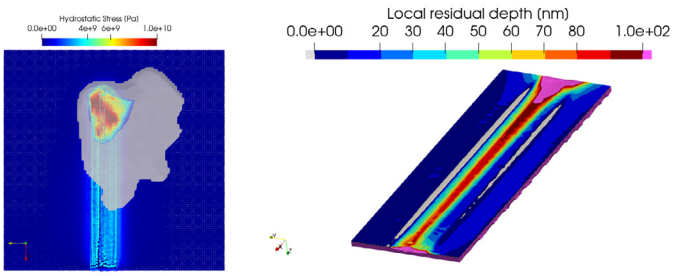

Fig. 11. Grinding of silicon: hydrostatic stress field under the diamond grain (topview, left) and residual scratch depths (right) for a scratch depth of 500nm, from [31].

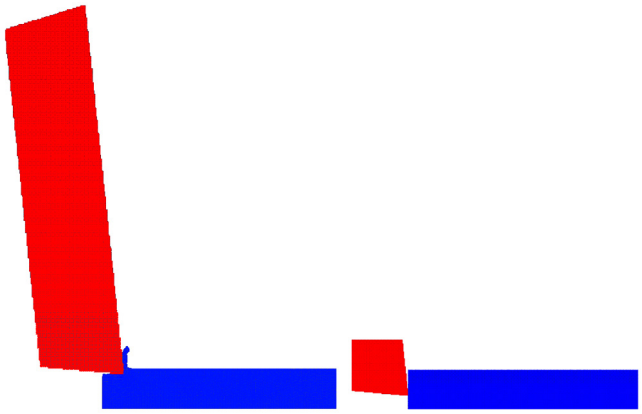

Fig. 12. Orthogonal cutting simulation using the SPH with the workpiece coloured in blue and the tool in red. When using a full-scale (left) instead of a reduced tool model (right), the total number of particles increases by a factor of 3, thus leading to much higher runtimes.

cation of friction law and material constitutive model parameters. Secondly, it was shown that parallelisation allows for high-resolution simulations of chip formation and that chip segmentation during the machining of Ti6Al4V can also be shown with the classical JC model when the particle spacing is chosen below the shear layer thickness, so that the use of JC extensions with tanh-term [21, 22, 23] is not necessarily required to represent shear localisation.

The 3D simulations shown with single and multiple diamond grains were only made possible by the GPU parallelisation, which also demonstrated the ability of obtaining results within a reasonable runtime. Using the CSPM correction scheme, it was possible to reproduce the experimentally observed chip curling in the SPH simulation and in a multiple grain simulation the effect of overlapping grain paths on tool wear were investigated. In another simulation diamond scratching in silicon in the ductile mode was analysed where the cutting forces could be reproduced with reasonable accuracy, but the normal force was overestimated. The framework iMFREE serves as a basis for further developments, of which two current research areas are briefly introduced.

During simulations with coupled tool-workpiece heat conduction, it became apparent that the particle discretisation can only represent the tool insufficiently accurately at the outer areas, which leads to significantly increased particle numbers, especially when using real tool geometries. The problem is illustrated in Figure 12. For this reason, iMFREE is being further developed in [32] so that the tool is discretised by means of an FEM mesh, thus greatly reducing the computational effort compared to a pure SPH description. A special feature here is that the FEM-SPH coupling is GPU parallelised, therefore maintaining the overall performance of the solver.

The coupled FEM-SPH solver allows the instantaneous modification of the tool geometry due to wear during the cutting simulation. Several wear models, which are available in the literature, are investigated and compared with orthogonal cutting experiments, and insights for wear model calibration are provided for numerical modelling methods. The progress of the work can be found in the publication [33] at this conference.

Acknowledgements

The authors would like to thank the Swiss National Science Foundation which financially supported parts of the presented work under Grant No. 200021-149436. Further, the authors would like to acknowledge Matthias Röthlin and his invaluable contribution to the development of iMFREE.

References

[1] P. Arrazola, T. Özel, D. Umbrello, M. Davies, I. Jawahir, Recent advances in modelling of metal machining processes, CIRP Annals-Manufacturing Technology 62 (2) (2013) 695–718.
[2] P. Sridhar, J. M. R. Prieto, K. M. de Payrebrune, Discretization approaches to model orthogonal cutting with lagrangian, arbitrary lagrangian eulerian, particle finite element method and smooth particle hydrodynamics formulations, Procedia CIRP 93 (2020) 1496–1501.
[3] X. Ye, J. M. R. Prieto, R. Müller, An improved particle finite element method for the simulation of machining processes, in: 2nd International Conference of the DFG International Research Training Group 2057–Physical Modeling for Virtual Manufacturing (iPMVM 2020), Schloss Dagstuhl-Leibniz-Zentrum für Informatik, 2021.
[4] X. Gu, C. Dong, T. Cheng, Mpm simulations of high-speed machining of ti6al4v titanium alloy considering dynamic recrystallization phenomenon and thermal conductivity, Applied Mathematical Modelling 56 (2018) 517–538.
[5] M. Röthlin, H. Klippel, M. Afrasiabi, K. Wegener, Metal cutting simulations using smoothed particle hydrodynamics on the gpu, The International Journal of Advanced Manufacturing Technology 102 (9) (2019) 3445–3457.
[6] J. J. M. R. A. Gingold, Smoothed particle hydrodynamics: theory and application to non-spherical stars, Monthly Notices of the Royal Astronmical Society.
[7] W. K. L. Shaofan Li, Meshfree Particle Methods, Springer, 2004.
[8] L. D. L. A. Petschek, Smooth particle hydrodynamics with strength of materials, Unklar; Center for Explosives Technology Research and Department of Physics.
[9] M. Heinstein, D. Segalman, Simulation of orthogonal cutting with smooth particle hydrodynamics, Sandia National Laboratories, California.
[10] M. Röthlin, Meshless Software Tool to Simulate Metal Cutting Operations by Employing Contemporary Numerical Methods, ETH Zurich, 2019.
[11] M. Röthlin, H. Klippel, K. Wegener, Meshless methods for large deformation elastodynamics, arXiv preprint arXiv:1807.01117.

[12] M. Afrasiabi, M. Roethlin, K. Wegener, Contemporary meshfree methods for three dimensional heat conduction problems, Archives of Computational Methods in Engineering (2019) 1–35.
[13] H. Klippel, Constitutive equations for simulation of metal cutting with meshless methods on gpu, Ph.D. thesis, ETH Zurich (2021).
[14] H. Klippel, M. Gerstgrasser, D. Smolenicki, E. Cadoni, H. Roelofs, K. Wegener, Johnson cook flow stress parameter for free cutting steel 50sib8, arXiv preprint arXiv:2007.14087.
[15] M. Gerstgrasser, D. Smolenicki, M. Akbari, H. Klippel, H. Roelofs, E. Cadoni, K. Wegener, Analysis of two parameter identification methods for original and modified johnson-cook fracture strains, including numerical comparison and validation of a new blue-brittle dependent fracture model for free-cutting steel 50sib8, Theoretical and Applied Fracture Mechanics (2021) 102905.
[16] N. Rttimann, Simulation of metal cutting processes using meshfree methods, Ph.D. thesis, ETH Zrich (2012).
[17] M. Calamaz, J. Limido, M. Nouari, C. Espinosa, D. Coupard, M. Salaün, F. Girot, R. Chieragatti, Toward a better understanding of tool wear effect through a comparison between experiments and sph numerical modelling of machining hard materials, International journal of refractory metals and hard materials 27 (3) (2009) 595–604.
[18] M. Afrasiabi, L. Meier, M. Röthlin, H. Klippel, K. Wegener, Gpu-accelerated meshfree simulations for parameter identification of a friction model in metal machining, International Journal of Mechanical Sciences 176 (2020) 105571.
[19] G. Johnson, W. Cook, A constitutive modeling and data for metals subjected to large strain rates and high temperatures, Proceedings of 7th international symposium on ballistics (1983) 541–577.
[20] H. Klippel, S. Süssmaier, M. Kuffa, K. Wegener, Dry cutting experiments database ti6al4v and ck45, arXiv preprint arXiv:2209.04197doi:10.48550/ARXIV.2209.04197.
URL https://doi.org/10.48550/arXiv.2209.04197
[21] M. Calamaz, D. Coupard, F. Girot, A new material model for 2d numerical simulation of serrated chip formation when machining titanium alloy ti–6al–4v, International Journal of Machine Tools and Manufacture 48 (3-4) (2008) 275–288.
[22] M. Calamaz, D. Coupard, F. Girot, Numerical simulation of titanium alloy dry machining with a strain softening constitutive law, Machining Science and Technology 14 (2) (2010) 244–257.
[23] M. Sima, T. Özel, Modified material constitutive models for serrated chip formation simulations and experimental validation in machining of titanium alloy ti–6al–4v, International Journal of Machine Tools and Manufacture 50 (11) (2010) 943–960.
[24] H. Klippel, E. G. Sanchez, M. Isabel, M. Röthlin, M. Afrasiabi, K. Michal, K. Wegener, Cutting force prediction of ti6al4v using a machine learning model of sph orthogonal cutting process simulations, Journal of Machine Engineering 22.
[25] P. L. B. Oxley, The mechanics of machining: an analytical approach to assesing machinability, Ellis Horwood, 1989.
[26] D. Lalwani, N. Mehta, P. Jain, Extension of oxley's predictive machining theory for johnson and cook flow stress model, Journal of materials processing technology 209 (12-13) (2009) 5305–5312.
[27] C.-F. Wyen, K. Wegener, Influence of cutting edge radius on cutting forces in machining titanium, CIRP annals 59 (1) (2010) 93–96.
[28] M. Röthlin, H. Klippel, M. Afrasiabi, K. Wegener, Meshless single grain cutting simulations on the gpu, International Journal of Mechatronics and Manufacturing Systems 12 (3-4) (2019) 272–297.
[29] N. Rttimann, S. Buhl, K. Wegener, Simulation of single grain cutting using sph method, Journal of Machine Engineering 10.
[30] N. Rüttimann, M. Roethlin, S. Buhl, K. Wegener, Simulation of hexa-octahedral diamond grain cutting tests using the sph method, Procedia CIRP 8 (2013) 322–327.
[31] H. Klippel, S. Süssmaier, M. Röthlin, M. Afrasiabi, U. Pala, K. Wegener, Simulation of the ductile machining mode of silicon, The International Journal of Advanced Manufacturing Technology 115 (5) (2021) 1565–1578.
[32] N. Zhang, H. Klippel, M. Afrasiabi, M. Röthlin, M. Kuffa, M. Bambach, K. Wegener, Hybrid sph-fem solver for metal cutting simulations on the gpu including thermal contact modeling, CIRP Journal of Manufacturing Science and Technology.
[33] N. Zhang, H. Klippel, M. Afrasiabi, M. Röthlin, M. Kuffa, M. Bambach, K. Wegener, Study on the effect of wear models in tool wear simulation using hybrid sph-fem method, Procedia Cirp.